

Competing mechanisms for the reaction of dichloropropynylborane with 2-*tert*-butylbutadiene. Diels-Alder reaction *versus* Alkynylboration

Margarita M. Vallejos,^{*a} and Silvina C. Pellegrinet^{*b}

Área de Química Orgánica, Departamento de Química, Facultad de Ciencias Exactas y Naturales y Agrimensura, Universidad Nacional del Nordeste, Avda. Libertad 5460, (3400) Corrientes, Argentina.

^bInstituto de Química Rosario (CONICET), Facultad de Ciencias Bioquímicas y Farmacéuticas, Universidad Nacional de Rosario, Suipacha 531, Rosario (2000), Argentina. E-mail: vallejos.marga@gmail.com, pellegrinet@iquir-conicet.gov.ar

Supporting Information

List of contents:

- MPWB1K/6-311++G(d,p) energies in DCM for reactants and products. Page S2.
- Topological analysis of charge density properties along the reaction paths. Pages S3-S10.
- Cartesian coordinates and absolute energies (in hartrees), including ZPE of all stationary points reported in the paper and values of imaginary frequencies of all transition structures. Pages S11-S16.
- References. Page S17.

Table S1. MPWB1K/6-311++G(d,p) absolute total energies (E , in a.u.) and free energies (G , in a.u.) and relative energies (ΔE , in kcal mol⁻¹) and free energies (ΔG , in kcal mol⁻¹) in DCM

Species	E	ΔE^a	G	ΔG^a
1	-313.13095		-312.96274	
2	-1061.52240		-1061.50106	
3	-1374.741492	-55.31	-1374.520023	-35.28
4	-1374.741573	-55.36	-1374.520132	-35.35
5	-1374.682483	-18.28	-1374.467729	-2.46
6	-1374.678666	-15.88	-1374.466575	-1.74

^a Relative to **1 + 2**.

Topological analysis of charge density properties along the reaction paths

The topological concepts of the quantum theory of atoms in molecules (QTAIM) are well documented in the standard literature^{1,2} thus, we only give the theoretical information needed for the discussion of our results.

In accordance with the QTAIM theory, a bond between two atoms is characterized by a line of maximum electron density, the bond path, that connects the respective nuclei and intersects the zero-flux surface of the electron density gradient field ($\nabla\rho_r$) at the bond critical point (bcp). Several topological properties evaluated at the bcp are used to characterize the nature of a bonding interaction (calculated properties at the bcp in ρ_r topology are labeled with the subscript “b”): (1) the charge density, ρ_b , as a measure of accumulation of electron charge between the bonded nuclei, which reflects the bond strength; (2) the Laplacian of electron charge density, $\nabla^2\rho_b$, gives information about the local charge concentration ($\nabla^2\rho_b < 0$) or depletion ($\nabla^2\rho_b > 0$); and (3) the ellipticity, defined as $\varepsilon = (\lambda_1/\lambda_2) - 1$, gives an idea about the charge distribution around the bond path and also is employed to determine the π character of a bond and its stability.³ ρ_b and $\nabla^2\rho_b$ are employed to analyze the covalent character of an interaction.⁴ The delocalization index (*DI*) indicates the extent of exchange of electrons between two atomic basins, and it can be calculated between two atoms bonded by a bond path or without having a bond path.⁵ Another critical points often found in a molecular system are ring critical point (rcp) and cage critical point (ccp).

In the QTAIM context, an atom in a molecule might be defined as a region of space bounded by one or more zero-flux surfaces. The atomic electron population $N(\Omega)$ can be obtained by integrating the electron density over the atomic basin, which can be used to calculate the corresponding atomic net charge as $q(\Omega) = N(\Omega) - Z\Omega$, ($Z\Omega$) being the atomic number.

Moreover, the contour plot of the Laplacian function for the atomic system exhibits a shell of charge concentration and another one of charge depletion for each quantum shell. The outer quantum shell of an atom over $\nabla^2\rho_r < 0$ is called valence shell charge concentration (VSCC). According to some authors, it is convenient to consider the $-\nabla^2\rho_r$ function for a more intuitive interpretation.⁶ For an isolated atom, the VSCC is located at a sphere in which the valence electronic charge is concentrated in a maximum and uniform way.

We carried out an analysis of the changes in the topological properties along the reaction coordinates associated with **TSC-m** and **TSC-D**. Fig. S1 shows the contour lines of the $-\nabla^2\rho_r$ superimposed on the molecular graphs for selected structures along the reaction paths. The variation of several topological properties (ρ_b , $\nabla^2\rho_b$ and ε) at the selected bcps are displayed in Fig. S2 in which the energy profiles are also included. Fig. S3 shows the changes of the *DI* of selected interactions and Fig. S4 displays the variation of the atomic net charges.

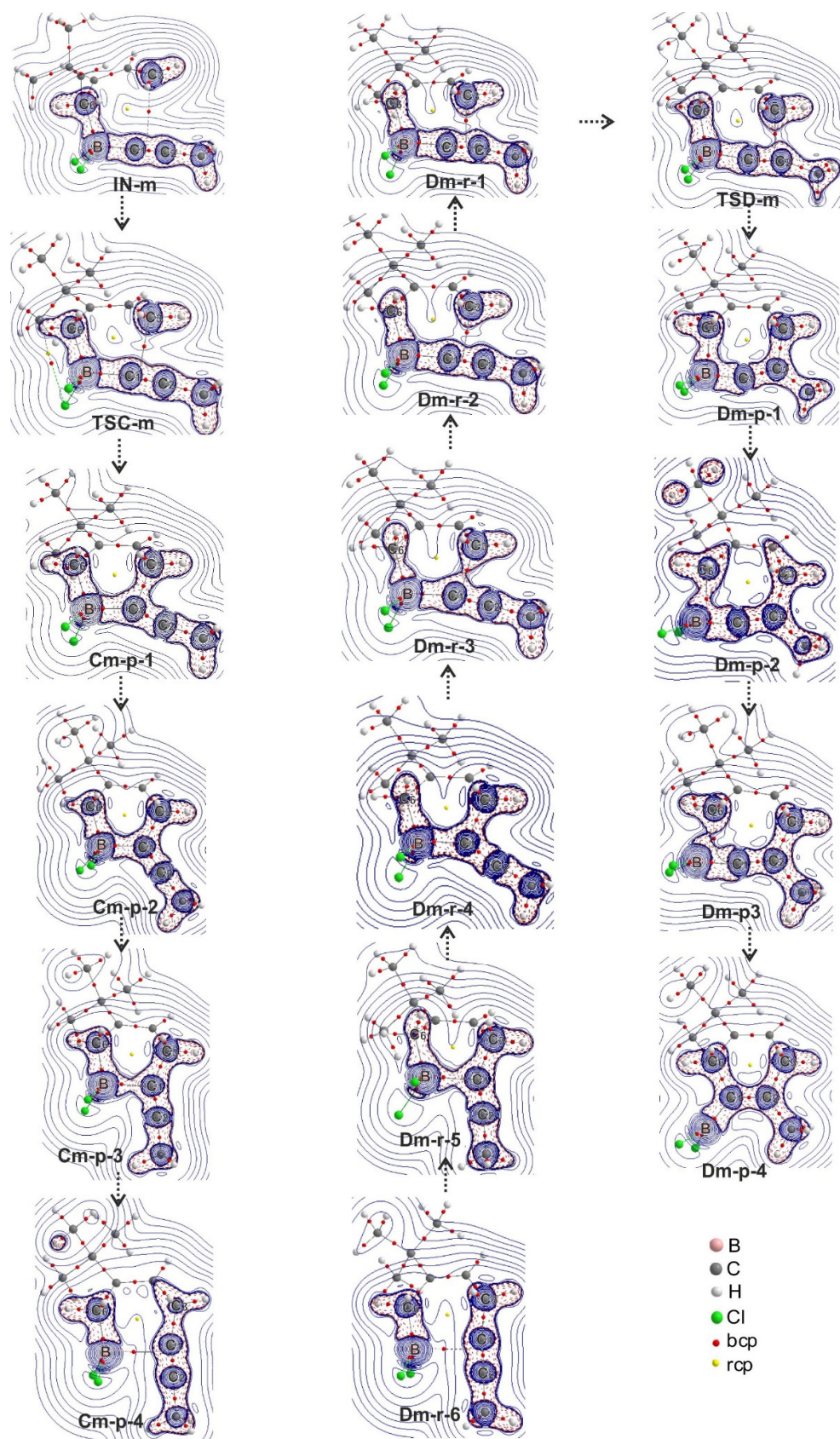


Fig. S1 Contour plots of $-\nabla^2\rho_r$ superimposed on the molecular graphs of selected structures along the reaction coordinate associated with **TSC-m** and **TSD-m**. Continuous blue lines and dashed red lines depict regions of local charge density depletion and concentration, respectively.

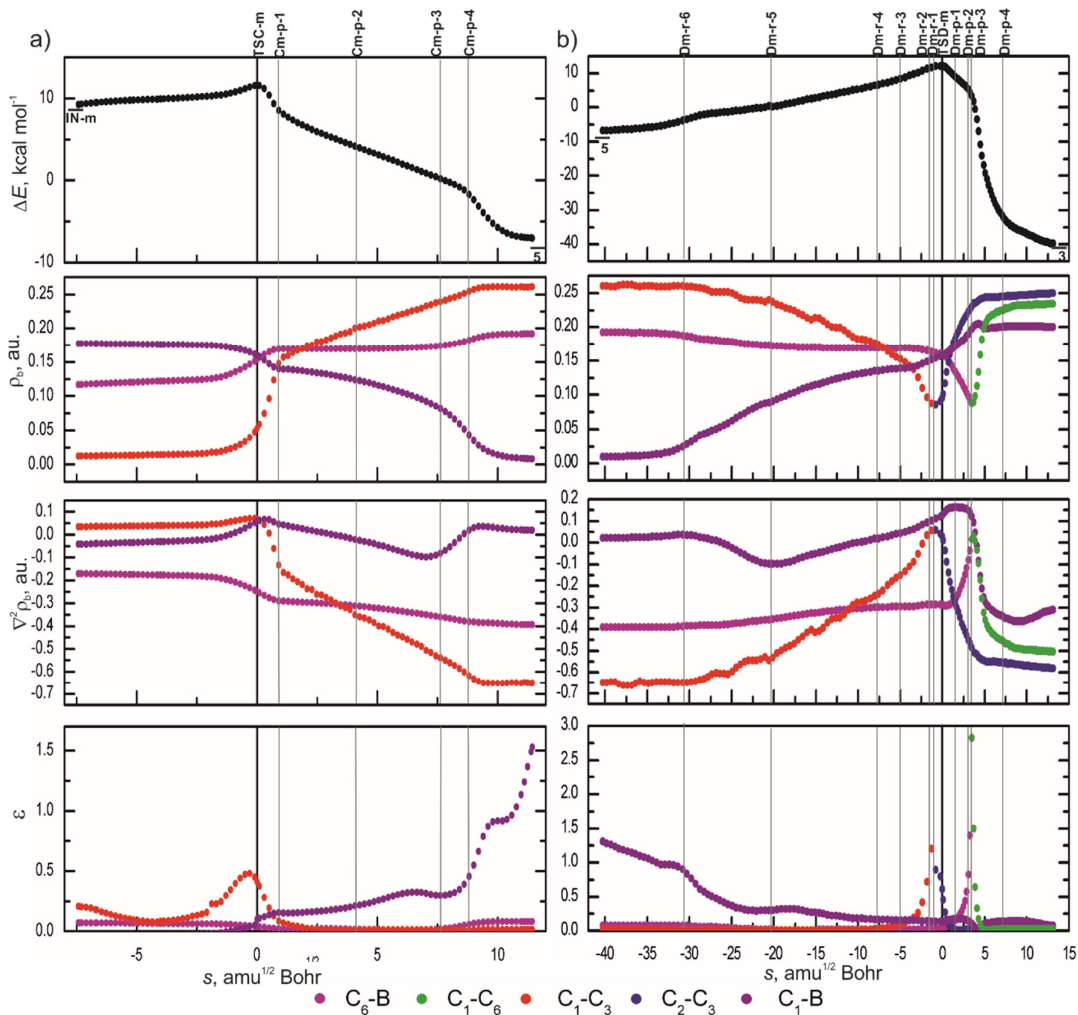


Fig. S2 Relative energy (ΔE), topological properties (ρ_b : charge density, $\nabla^2 \rho_b$: Laplacian of the charge density and ε : ellipticity) along the IRC paths associated with (a) **TSC-m** and (b) **TSD-m**. TSs are located at $s = 0.0 \text{ amu}^{1/2} \text{ Bohr}$.

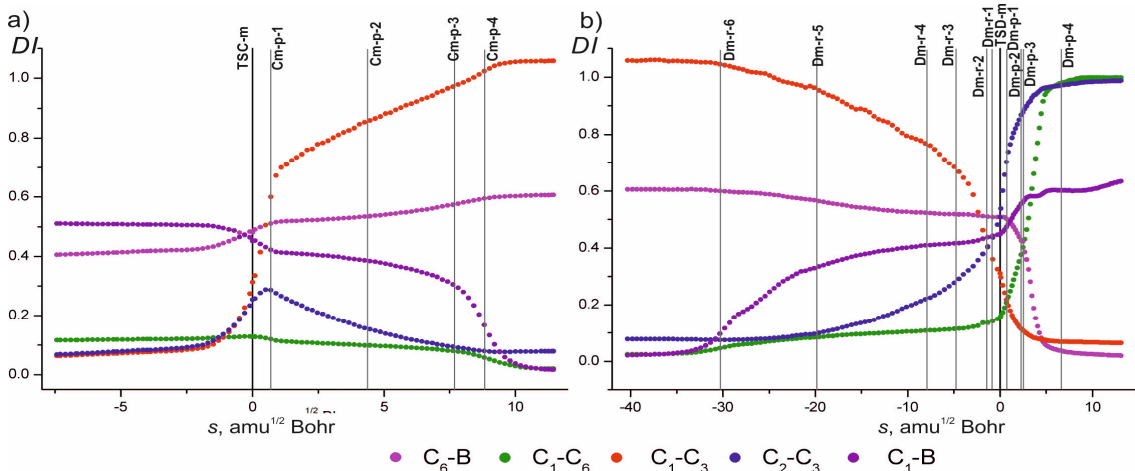


Fig. S3 Evolution of the delocalization indices (DI) along the IRC paths associated with a) **TSC-m** and b) **TSD-m**. TSs are located at $s = 0.0 \text{ amu}^{1/2} \text{ Bohr}$.

In the pathway associated with **TSC-m** the topological properties at the C₁-C₃ and C₁-B bcps show larger variations. The C₁-C₃ bond-forming and the C₁-B bond-breaking begin after **TSC-m**. The topological properties at the C₁-C₃ bcp show important changes from **TSC-m** to **Cm-p-1** on the IRC, the values of ρ_b increase from 0.052 au. to 0.147 au., $\nabla^2\rho_b$ varies from 0.079 to -0.133 au., ε decreases from 0.42 to 0.08 and DI C₁-C₃ increase from 0.31 to 0.67. In this stage of the reaction, the C₁-C₃ interaction shows features of a shared-shell interaction, and the formation of the C₁-C₃ covalent bond occurs. In contour plot of the $-\nabla^2\rho_t$ for **TSC-m** the C₁-C₃ bcp is localized in a region of the charge depletion while that for **Cm-p-1** it appears in a region of charge concentration (See Fig. S1). After **Cm-p-1**, ρ_b and DI at the C₁-C₃ bcp increase progressively and $\nabla^2\rho_b$ becomes more negative indicating that the C₁-C₃ covalent bond is reinforced.

The C₁-B bond-breaking occurs more delayed. ρ_b at the C₁-B bcp decreases from 0.160 au. at **TSC-m** to 0.140 au. at **Cm-p-1**, then this undergoes a smooth and continuous decrease and after **Cm-p-3** the values of ρ_b fall down abruptly denoting the C₁-B bond-breaking. Also, from **Cm-p-3** to the end of the reaction ε at the C₁-B bcp increases abruptly reflecting the instability of the C₁-B interaction. In contour plot of the $-\nabla^2\rho_t$ for **Cm-p-3**, it can be visualized that the region of charge concentration around the C₁-B bcp is slimmer while in **Cm-p-4** this bcp is already located in a region of the charge depletion (See Fig. S1).

From **IN-m** to nearly before **TSC-m** the values of ρ_b , $\nabla^2\rho_b$ and DI at the C₆-B bcp remain practically constant ($\rho_b \sim 0.13$ au., $\nabla^2\rho_b \sim -0.18$ au. and $DI \sim 0.4$) then, ρ_b and DI increase and $\nabla^2\rho_b$ becomes more negative up to *ca.* 0.18 au., 0.5 and -0.30 au., respectively at **Cm-p-1**. These results demonstrate that the C₆-B covalent bond is almost formed since an early stage of the reaction.

In the IRC associated with **TSC-D**, from **5** to the TS the topological properties change in a reverse manner than those from **TSC-m** to **5**. ρ_b and DI at the C₁-B bcp increase from values close to zero, up to 0.157 au. and 0.45 at **TSD-m** and, consequently, the C₁-B bond is formed.

At the C₁-C₃ bcp, ρ_b and DI decrease progressively and $\nabla^2\rho_b$ becomes less negative while ε remains close to zero from enyne **5** until nearly **Dm-r-3**. Also, the contour plots of $-\nabla^2\rho_t$ show that the charge concentration around the C₁-C₃ bcp becomes narrower (See Fig. S1). Then after **Dm-r-3**, ρ_b and DI at the C₁-C₃ bcp decrease more sharply, $\nabla^2\rho_b$ reaches positive values and ε begins to increase, which denote an instability of the C₁-C₃ bonding interaction. At **Dm-r-2**, ρ_b at C₁-C₃ bcp is low (0.087 au.), $\nabla^2\rho_b$ is 0.056 au., and ε shows a relatively high value (1.20). Interesting, DI C₁-C₃ (0.41) has a similar value to DI C₂-C₃ (0.40), indicating that C₁ and C₂ are sharing equivalent amount of electrons with C₃ at **Dm-r-2**. In the following structure, **Dm-r-1**, a sudden change of the topological pattern occurs since the C₁-C₃ bcp disappears and the C₂-C₃ bcp appears leading from a six-membered ring to a seven-membered ring structure. At **Dm-r-1**, ε decrease significantly (0.79) at the new C₂-C₃ bcp and the C₂-C₃ becomes stronger since DI C₂-C₃ (0.41) is greater than DI C₁-C₃ (0.36). These results suggest that

there is a conflict structure between **Dm-r-2** and **Dm-r-1**, in which C_3 and the C_1 - C_2 bcp are connected through a bond path, i.e. wherein C_1 and C_2 are competing to become attached to C_3 .⁷ The conflict structure is a key species for the rearrangement of the six-membered ring zwitterion towards the seven-membered zwitterionic structure, which is involved in the pathway for the formation of the cycloadduct. In **TSD-m**, the C_6 -B bcp shows features of a closed shell interaction ($\rho_b = 0.160$ au., $\nabla^2\rho_b = -0.287$ au. and $DI = 0.51$) while the C_2 - C_3 interaction displays features of open shell interaction (ρ_b is 0.095 au., $\nabla^2\rho_b = 0.026$ au. and the $DI = 0.51$). In agreement with these results, in the contour plot of $-\nabla^2\rho$ it can be observed that the C_6 -B/ C_2 - C_3 bcps are placed in a region of the charge concentration/charge depletion. In addition, $DI_{C_1-C_6}$ and $DI_{C_1-C_3}$ are 0.15 and 0.31, respectively indicating that these atoms are sharing their electrons in **TSD-m**. This topological pattern is typical of [4 + 3] TS. Notably, **TSB-m**, which connects with **IN-m** and cycloadduct **3**, has a similar topological pattern to **TSD-m** (two new bcps, C_6 -B and C_2 - C_3 , and a ring critical point (rcp) related to the seven-membered cyclic structure) but differs in the values of the topological properties (See Fig. S4). For **TSB-m**, ρ_b and DI at the C_6 -B and C_2 - C_3 bcps are lower (0.142 au./0.47 and 0.077 au./ 0.46 at the C_6 -B and C_2 - C_3 bcps, respectively) than those for **TSD-m**. Also, $DI_{C_1-C_3}$ is 0.18 indicating that there are less electrons sharing between both atoms in **TSB-m** than in **TSD-m** while that $DI_{C_1-C_6}$ is 0.18, a little higher than in **TSD-m**. Therefore, the charge density among the atoms of the diene and the dienophile in **TSD-m** is higher due to the proximity to the conflict structure, in which the C_1 and C_2 atoms are closer to C_3 facilitating the sharing of their electrons. Consequently, **TSD-m** is more stabilized.

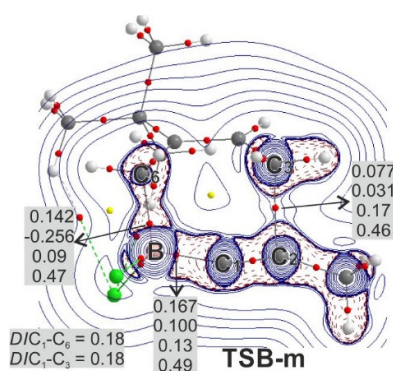


Fig. S4. Contour plot of $-\nabla^2\rho$ superimposed on the molecular graph of **TSB-m**. Continuous blue lines and dashed red lines depict regions of local charge density depletion and concentration, respectively. The values given for selected bcp, from top to bottom, are ρ_b , $\nabla^2\rho_b$, ϵ and DI . Also, DI of other interactions are included. All symbols are explained in the text. See Fig. 1 for key.

After **TSD-m**, ρ_b and DI increase abruptly, $\nabla^2\rho_b$ becomes negative and ϵ reaches values close to zero at the C_2 - C_3 bcp. At **Dm-p-1** ρ_b is 0.210 au., $\nabla^2\rho_b$ is -0.390 au. and is DI 0.88 denoting the shared-shell nature of the C_2 - C_3 interaction which can be also seen in Fig. S1. Hence, at **Dm-p-1** the C_2 - C_3 covalent bond is almost completely formed, and it is involved in a seven-membered ring structure. Also, at this point the C_1 - C_3 interaction becomes negligible being $DI_{C_1-C_3}$ close to zero. Then, ρ_b and DI at the C_2 -

C_3 bcp increase slightly and $\nabla^2\rho_b$ becomes a little more negative (0.245 au., 0.98, and -0.556 au., respectively) at **Dm-p-4**, closer to the end of the reaction coordinate.

The most important changes from **TSD-m** to cycloadduct **3** occur in the region among C_6 , B and C_1 . ρ_b and DI decrease and $\nabla^2\rho_b$ becomes less negative at the C_6 -B bcp. At **Dm-p-2**, ρ_b at the C_6 -B bcp is relatively low (0.091 au.), $\nabla^2\rho_b$ has a small negative value (-0.036 au.) and ε increases up to 1.40 reflecting an instability of the C_6 -B bonding interaction and, the asymmetrical distribution of the charge density around the C_6 -B bcp, as it can be seen clearly visualized in the contour plot of $-\nabla^2\rho_b$ of this structure (See Fig. S1). Suddenly, at **Dm-p-3** the C_6 -B bcp disappears and the C_1 - C_6 bcp appears. ρ_b at the C_1 - C_6 bcp is 0.088 au., $\nabla^2\rho_b$ is 0.016 au. and ε reaches a maximum value of 2.82. Furthermore, DI C_1 - C_6 increases (0.61) and DI C_6 -B decreases (0.23). Therefore, an important rearrangement of the charge density occurs between C_1 and C_6 due to the rearrangement of these atoms to form the corresponding C_1 - C_6 σ -bond. These findings also suggest that the system passes through a conflict structure, in which the B and C_1 atoms are competing to be bound to C_6 .⁷ This constitutes a key point in the evolution of the [4 + 3] structure towards the [4 + 2] structure.⁸

After the conflict species, at **Dm-p-4**, ρ_b at the C_1 - C_6 bcp increases, $\nabla^2\rho_b$ becomes more negative (*ca.* 0.229 au. and -0.478), and ε decreases abruptly towards values nearly zero. In this part of the IRC the C_1 - C_6 bond is reinforced showing features of a covalent bond. At **Dm-p-4**, both C_1 - C_6 and C_2 - C_3 covalent bonds are almost completely formed.

The variations of the atomic charges of selected atoms along the reaction coordinates associated with **TSC-m** and **TSD-m** are shown in Fig. S5.

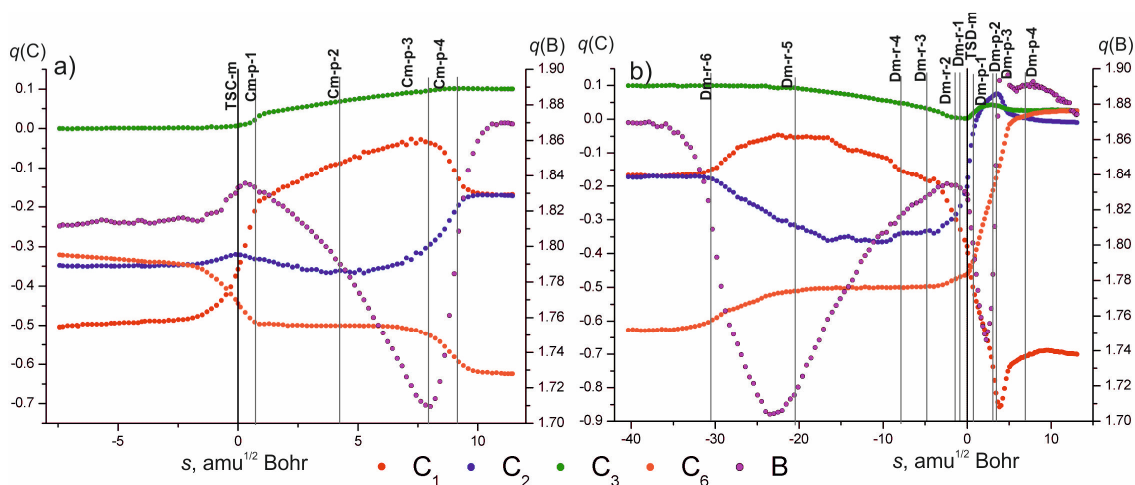


Fig. S5 Atomic net charges for selected atoms (in e) along the reaction coordinates associated with **TSC-m** and **TSD-m**.

In path C, before **TSC-m** the negative charge of C_1 is $\sim -0.50 e$ then, it changes up to $-0.03 e$ at **Cm-p-3**. After **Cm-p-3**, $q(C_1)$ becomes less negative up to $\sim -0.15 e$ and then remains constant. The electron

charge of C₂ is -0.32 *e* at **TSC-m** and then decreases slightly at **Cm-p-1** (-0.33 *e*) and **Cm-p-2** (-0.36 *e*). From **Cm-p-3** onwards *q*(C₂) increases reaching similar value *q*(C₁). Therefore, firstly C₂ gains electron population and C₁ loses electron population after **TSC-m** but after **Cm-p-3**, both atoms exhibit similar net charges. The electron charge of B undergoes remarkable changes during the course of the reaction. At **TSC-m**, *q*(B) is +1.83 *e* then decreases abruptly to a minimum of +1.71 *e* at **Cm-p-3**. The B atom in this stage of the reaction is tetracoordinated. Then, *q*(B) increases (passing by **Cm-p-4** in which *q*(B) = +1.81 *e*) up to a maximum of +1.87 *e*. In this part of the reaction coordinate the C₁-B bond breaking occurs, and the B atom becomes tricoordinated *q*(C₃) remains close to zero along the reaction coordinate.

From enyne **5** to **TSD-m**, the changes in the net charges of the analyzed atoms are almost opposite to those observed from **TSC-m** to the enyne. The negative charges of C₁ and C₂ are practically similar (-0.15 and -0.17 *e*, respectively) at **Dm-r-6**. Firstly, *q*(C₁) and *q*(C₂) change to -0.05 and -0.30 *e*, respectively at **Dm-r-5**. Then, C₁ increases and C₂ decreases their negative atomic charges becoming similar at **Dm-r-2** (*q*(C₁) = -0.30 *e* and *q*(C₂) = -0.28 *e*). After this point, the charges of C₁ and C₂ undergo striking variations. *q*(C₁) becomes more negative (-0.38, -0.66, -0.78 *e* at **TSD-m**, **Dm-p-1** and **Dm-p-2**, respectively) down to a maximum negative value of -0.82 *e* at **Dm-p-3**, then it falls to ~ -0.70 *e*, remaining constant until the end of the reaction. The negative charge of C₂ decreases becoming positive (+0.06, +0.07 *e* at **Dm-p-1** and **Dm-p-2**, respectively) up to a maximum value of +0.08 *e* at **Dm-p-3**, then it decreases to values close to zero until the final product. The maximum values of *q*(C₁) and *q*(C₂) occur at the same point of the reaction coordinate in which the ρ_b goes down to a minimum, $\nabla^2\rho_b$ becomes positive and the ε is a maximum at the C₆-B bcp, demonstrating that an important redistribution of the charge density occurs in this stage. In addition, these results reveal that a charge transfer process between C₁ and C₂ occur along the reaction coordinate. The notable variations in the net charges of C₁ and C₂ are attributed to the changes of their hybridization (from “*sp*” in the enyne to “*sp*²” hybridization in the cycloadduct).

q(B) undergoes significant variations during the course of the reaction. Close to the enyne *q*(B) is +1.87 *e*, then it decreases abruptly to +1.70 *e* (close to **Dm-r-5**). Then, *q*(B) increases to ~ +1.83 *e* near the conflict structure (**Dm-r-1** and **Dm-r-2**). In this part of the reaction coordinate, the boron atom is tricoordinated (in the enyne product) and then the C₁-B bond formation occurs, becoming tetracoordinated.

At **TSD-m** *q*(B) is +1.83 *e*, then it decreases abruptly up to a minimum of + 1.74 *e* (close to **Dm-p-1**). Afterwards, *q*(B) increases again up to ~ +1.89 *e* at the end of the reaction. In this part of the reaction coordinate, firstly B gain electron population becomes less positive (in this stage the B atom is tetra-coordinate), then the C₆-B bond begins breaking and the B atom losses electron population, which is donated to C₁ for the formation of the C₁-C₆ σ -bond. The B atom becomes tricoordinated and its charge gets more positive.

From **TSD-m** afterwards, $q(C_6)$ undergoes significant changes. The negative charge of C_6 goes sharply from $-0.46 e$ at **TSD-m** up to $-0.18 e$ at **Dm-p-3**, and then remains close to zero. These results show that the C_6 loses electron charge, which could be donated to C_1 and/or B, and in this part of the reaction the C_6 -B bond is broken and C_6 begins to form a new bond with C_1 .

B3LYP/6-311++G(d,p) Cartesian coordinates, imaginary frequencies of transition structures, and computed absolute electronic energies (including zero-point energy -ZPE- corrections) and free energy of the stationary points involved in reaction of 2-*tert*-butylbutadiene (**1**) with dichloropropynylborane (**2**).

2-*tert*-butylbutadiene (**1**)

C	-0.767303	1.775564	-0.129730
C	-0.508440	0.459776	-0.127175
C	-1.614550	-0.511260	-0.306174
C	-2.842796	-0.393690	0.207422
C	0.906115	-0.126777	0.029067
H	-1.772981	2.143566	-0.298763
H	0.000901	2.522204	0.021069
H	-1.391583	-1.400762	-0.890380
H	-3.121924	0.441001	0.842221
H	-3.604991	-1.140073	0.012919
C	1.324921	-0.820649	-1.290052
C	0.907958	-1.164821	1.175074
C	1.951173	0.954533	0.353012
H	2.330617	-1.238867	-1.185836
H	1.338068	-0.106861	-2.118437
H	0.655687	-1.641034	-1.559139
H	1.907467	-1.594243	1.292092
H	0.211556	-1.984713	0.983763
H	0.625236	-0.698922	2.123635
H	2.932168	0.488137	0.478493
H	1.711459	1.483091	1.279652
H	2.035849	1.691421	-0.449946

Energy + ZPE = -313.137193 au.

Free Energy = -313.170851 au.

dichloropropynylborane (**2**)

B	-0.544176	0.000135	-0.000002
C	0.946511	0.001727	-0.000012
Cl	-1.459495	1.515343	0.000002
C	2.160481	0.003965	-0.000035
Cl	-1.456543	-1.516839	0.000002
C	3.610565	0.001938	-0.000008
H	3.989398	-0.517144	0.885061
H	4.009198	1.019137	-0.003285
H	3.989573	-0.523024	-0.881516

Energy + ZPE = -1061.459765 au.

Free Energy = -1061.493790 au.

TSA-m

1 imaginary frequency : -419.7 cm⁻¹

C	-1.618629	0.815785	0.261300
C	-1.310192	2.025997	0.347421
C	-1.694641	3.316210	0.976246
B	-1.870775	-0.622918	0.131457
Cl	-1.416627	-1.785248	1.431585
Cl	-2.923319	-1.288255	-1.174814
H	-0.877438	3.712376	1.584513
H	-1.938197	4.066402	0.219408
H	-2.567427	3.170118	1.615152
C	0.253856	2.511894	-0.825955
C	1.306256	1.695628	-0.424493
C	1.361340	0.294237	-0.642438
C	0.339092	-0.303335	-1.340201
C	2.505070	-0.508114	0.011891
C	2.412278	-2.011535	-0.302711
C	3.851814	0.019806	-0.536469
C	2.471913	-0.331283	1.548369
H	0.340596	3.571324	-0.614122
H	-0.300555	2.288672	-1.729278
H	2.042584	2.137391	0.238499
H	0.294276	-1.374116	-1.481282
H	-0.328676	0.274254	-1.961947
H	1.495892	-2.455062	0.094792
H	3.256849	-2.531728	0.156568
H	2.449567	-2.203345	-1.378651
H	4.680550	-0.532501	-0.083715
H	3.998153	1.079466	-0.313675
H	3.909802	-0.108756	-1.621018
H	1.528693	-0.694338	1.963889
H	2.592789	0.713111	1.845315
H	3.286537	-0.900872	2.005393

Energy + ZPE = -1374.563093 au.

Free Energy = -1374.607669 au.

TSA-p

1 imaginary frequency : -414.3 cm⁻¹

C	-1.256982	0.992434	0.231024
C	-0.260570	1.750328	0.222687
C	0.283471	3.009510	0.793686
B	-2.346515	0.013175	0.224780
Cl	-2.504558	-1.232429	1.518637
Cl	-3.750582	0.153281	-0.899318
H	0.503987	3.736746	0.008035

H	-0.445747	3.447882	1.477577
H	1.209433	2.824916	1.344104
C	1.181190	1.160441	-1.084454
C	1.550983	-0.134376	-0.717806
C	0.625345	-1.191370	-0.940178
C	-0.599695	-1.039094	-1.524496
C	2.829974	-0.437570	0.080037
C	3.608692	-1.568399	-0.635526
C	3.762302	0.782613	0.189081
C	2.457774	-0.898284	1.511527
H	1.893312	1.964415	-0.962628
H	0.512499	1.298280	-1.924148
H	0.849491	-2.160935	-0.508322
H	-1.280710	-1.879808	-1.584544
H	-0.861212	-0.175844	-2.119822
H	4.522704	-1.795283	-0.079175
H	3.892785	-1.267182	-1.647583
H	3.027390	-2.489936	-0.707287
H	3.303169	1.606570	0.740861
H	4.062797	1.152497	-0.795113
H	4.669739	0.497549	0.727504
H	1.904604	-0.119308	2.042536
H	3.367283	-1.117171	2.078739
H	1.843515	-1.801154	1.503450

Energy + ZPE = -1374.563762 au.
Free Energy = -1374.608561 au.

IN-m

C	1.299498	0.469636	-0.613831
C	1.125857	1.897824	-0.642632
C	0.114739	2.536506	-1.268898
C	0.275667	-0.395383	-1.096546
C	2.604117	-0.051372	-0.023581
C	2.734440	0.400160	1.457780
C	2.741441	-1.582433	-0.091398
C	3.765547	0.575150	-0.849852
H	1.847001	2.501162	-0.105974
H	0.025551	3.614668	-1.203119
H	-0.612061	2.031326	-1.889510
H	-0.288133	0.023893	-1.927679
H	0.604689	-1.407416	-1.306741
H	1.934176	-0.021878	2.066838
H	3.690198	0.038588	1.844997
H	2.720593	1.485558	1.567133
H	2.733312	-1.943476	-1.123032
H	3.698861	-1.870545	0.348719
H	1.951523	-2.088137	0.464080
H	3.691083	0.302682	-1.905494
H	3.796160	1.662941	-0.774978
H	4.710143	0.184080	-0.463630
C	-2.366804	1.748538	0.558403

C	-1.807207	0.698145	0.317933
B	-1.093872	-0.629638	0.012884
C	-3.070615	2.984632	0.875361
Cl	-2.222988	-1.816000	-0.959377
Cl	-0.526170	-1.504084	1.592170
H	-2.432457	3.670370	1.439714
H	-3.958284	2.778426	1.480371
H	-3.398462	3.497255	-0.033356

Energy + ZPE = -1374.580216 au.
Free Energy = -1374.626536 au.

IN-p

C	-0.737929	-1.079278	-1.238727
C	0.529199	-1.088556	-0.654495
C	1.566126	-0.093884	-0.744424
C	2.846998	-0.315554	0.081973
C	1.350966	0.999584	-1.513977
C	2.487882	-0.360414	1.585435
C	3.870906	0.809929	-0.142476
C	3.496268	-1.654775	-0.340459
H	-0.907663	-0.440575	-2.099016
H	-1.212946	-2.054093	-1.306486
H	0.721710	-1.916443	0.021397
H	2.066819	1.807355	-1.579683
H	0.453557	1.113363	-2.106403
H	3.391832	-0.529834	2.176781
H	2.040358	0.582974	1.908404
H	1.785511	-1.163201	1.822355
H	4.769564	0.604107	0.443736
H	4.170030	0.884296	-1.191744
H	3.485561	1.781782	0.177265
H	4.407493	-1.822560	0.239949
H	2.838811	-2.510944	-0.168389
H	3.765471	-1.642114	-1.400187
B	-1.896320	-0.310431	0.001617
C	-1.487804	1.146410	0.226915
C	-1.147215	2.300007	0.386899
C	-0.773955	3.690342	0.610180
Cl	-3.554152	-0.475247	-0.870156
Cl	-1.873618	-1.375334	1.546480
H	0.225927	3.766981	1.046097
H	-0.780028	4.255357	-0.326094
H	-1.476977	4.172712	1.295359

Energy + ZPE = -1374.578911 au.
Free Energy = -1374.626085 au.

TS-m

1 imaginary frequency : -252.1 cm⁻¹

C	1.193557	0.532375	-0.550043
---	----------	----------	-----------

C	0.915953	1.959860	-0.432611
C	-0.000629	2.642981	-1.136408
C	0.320336	-0.308334	-1.213308
C	2.492138	0.037426	0.095568
C	2.476050	0.313589	1.621398
C	2.742900	-1.463569	-0.134154
C	3.665246	0.823798	-0.550231
H	1.507793	2.513292	0.286855
H	-0.145777	3.703101	-0.964573
H	-0.605941	2.193712	-1.913614
H	-0.392728	0.132294	-1.898762
H	0.644062	-1.309049	-1.463257
H	1.657503	-0.217015	2.109936
H	3.416888	-0.036578	2.054295
H	2.383636	1.376595	1.851559
H	2.828554	-1.700322	-1.198031
H	3.685534	-1.744994	0.341563
H	1.954824	-2.081704	0.297560
H	3.699183	0.662083	-1.630887
H	3.598853	1.897786	-0.367122
H	4.607350	0.468987	-0.123775
C	-2.584788	1.454891	0.548912
C	-2.014162	0.413087	0.301940
B	-1.305066	-0.889692	-0.009899
C	-3.297782	2.682613	0.870035
Cl	-2.150636	-1.994624	-1.226458
Cl	-0.631187	-1.827213	1.418559
H	-2.663785	3.369503	1.437158
H	-4.182557	2.464771	1.475203
H	-3.629975	3.194918	-0.036933

Energy + ZPE = -1374.579328 au.
Free Energy = -1374.625992 au.

TS-p

1 imaginary frequency : -185.9 cm⁻¹

C	-0.717369	-1.077529	-1.313733
C	0.518642	-1.093316	-0.703447
C	1.570263	-0.097032	-0.767961
C	2.823905	-0.337696	0.094257
C	1.401826	0.991547	-1.548838
C	2.421381	-0.392273	1.586527
C	3.866154	0.778754	-0.086431
C	3.475497	-1.679240	-0.318616
H	-0.919096	-0.390743	-2.126893
H	-1.250893	-2.020431	-1.356221
H	0.698354	-1.930005	-0.035554
H	2.139523	1.779845	-1.605293
H	0.520807	1.122588	-2.162846
H	3.305843	-0.578811	2.202015
H	1.977348	0.554033	1.905822
H	1.702158	-1.187541	1.796013

H	4.741011	0.561646	0.531221
H	4.203740	0.855842	-1.123668
H	3.477502	1.752410	0.223738
H	4.367564	-1.859169	0.287628
H	2.806481	-2.531408	-0.174401
H	3.776727	-1.660057	-1.369642
B	-1.954732	-0.268100	0.054509
C	-1.479891	1.161686	0.256062
C	-1.094248	2.302502	0.402760
C	-0.663860	3.678054	0.608787
Cl	-3.562667	-0.427080	-0.859568
Cl	-1.899166	-1.377964	1.534969
H	0.330613	3.717758	1.061452
H	-0.629499	4.225627	-0.337046
H	-1.357170	4.201921	1.273100

Energy + ZPE = -1374.579419 au.
Free Energy = -1374.626736 au.

TSB-m

1 imaginary frequency : -269.1 cm⁻¹

C	1.138490	0.391035	-0.563050
C	0.774826	1.715403	-0.535099
C	-0.493922	2.170081	-0.991525
C	0.151286	-0.594003	-1.048613
C	2.513487	-0.023471	-0.008597
C	-1.983630	1.790158	0.324368
C	-1.813784	0.569467	0.203431
B	-1.210561	-0.825818	-0.075693
C	-2.596122	3.027747	0.827252
Cl	-2.420972	-1.931524	-1.039968
Cl	-0.761275	-1.680946	1.560504
C	2.605963	0.355893	1.491005
C	2.783736	-1.533411	-0.142658
C	3.611482	0.735184	-0.795694
H	1.414767	2.447218	-0.056619
H	-0.685824	3.235974	-0.927557
H	-0.944660	1.709869	-1.861012
H	-0.281828	-0.271391	-1.999461
H	0.569233	-1.588393	-1.188467
H	-1.854856	3.647894	1.336918
H	-3.389053	2.778684	1.534347
H	-3.029007	3.610541	0.010566
H	1.830859	-0.151236	2.069532
H	3.580969	0.053451	1.883858
H	2.500855	1.431698	1.645031
H	2.771695	-1.858429	-1.186492
H	3.775366	-1.755656	0.259923
H	2.057594	-2.128824	0.414439
H	3.567606	0.495303	-1.861625
H	3.519609	1.817730	-0.687034
H	4.596799	0.442144	-0.421923

Energy + ZPE = -1374.570257 au.

Free Energy = -1374.613635 au.

TSB-p

1 imaginary frequency : -207.1 cm⁻¹

C	0.888434	0.996766	-1.057300
C	1.320950	-0.292429	-0.612209
C	0.416949	-1.316759	-0.706423
C	-0.972757	-1.148833	-1.147470
C	2.724668	-0.443083	0.007160
C	3.788910	-0.063791	-1.049517
C	2.994982	-1.886317	0.467383
C	2.863642	0.490226	1.231124
B	-1.896327	-0.263985	-0.064171
Cl	-2.087277	-1.206289	1.579535
C	-1.169534	1.085327	0.172140
C	-0.409271	2.050508	0.277570
C	0.132588	3.358862	0.648451
Cl	-3.613316	0.018222	-0.827471
H	1.567825	1.836307	-0.969485
H	0.227487	1.067672	-1.909519
H	0.693235	-2.290220	-0.319601
H	-1.048918	-0.589058	-2.084559
H	-1.475191	-2.109171	-1.272739
H	3.727000	-0.722571	-1.920105
H	3.672305	0.966299	-1.397473
H	4.791946	-0.156027	-0.623255
H	2.304265	-2.199318	1.254705
H	2.923634	-2.598867	-0.358966
H	4.008589	-1.951380	0.870691
H	2.115359	0.257164	1.992872
H	3.854102	0.368944	1.678531
H	2.760929	1.543614	0.959496
H	1.054707	3.258992	1.225141
H	-0.601052	3.886680	1.261621
H	0.338113	3.965143	-0.237027

Energy + ZPE = -1374.569665 au.

Free Energy = -1374.613757 au.

TSC-m

1 imaginary frequency : -167.3 cm⁻¹

Cl	-0.862069	-1.593496	1.632641
B	-1.081445	-0.823138	-0.101304
C	0.364871	-0.679608	-0.896527
C	1.234521	0.433003	-0.437627
C	2.653529	0.152508	0.048570
C	0.713488	1.708274	-0.455547
C	-0.543347	1.992157	-1.026712
C	-1.812307	0.559034	0.069346

C	-2.471379	1.559482	0.330979
C	-3.295280	2.704185	0.674727
Cl	-2.196131	-1.995542	-1.132769
C	3.368075	1.410191	0.575260
C	2.662065	-0.918110	1.164016
C	3.448977	-0.383096	-1.174599
H	0.066786	-0.492467	-1.935562
H	0.872924	-1.642618	-0.878337
H	1.225001	2.521017	0.042606
H	-0.934831	2.999106	-0.941464
H	-0.896997	1.452942	-1.895062
H	-3.705660	3.182389	-0.218438
H	-4.135005	2.367645	1.290521
H	-2.731238	3.443650	1.248957
H	4.382616	1.144701	0.881664
H	3.447490	2.187330	-0.189144
H	2.860015	1.831390	1.446896
H	3.697339	-1.122588	1.450310
H	2.124121	-0.570907	2.048403
H	2.210280	-1.857308	0.843756
H	4.479530	-0.585309	-0.870415
H	3.024173	-1.310107	-1.564078
H	3.470802	0.352353	-1.983241

Energy + ZPE = -1374.573811 au.

Free Energy = -1374.618053 au.

TSC-p

1 imaginary frequency : -171.6 cm⁻¹

C	-0.912813	-1.350530	-1.120011
B	-1.778482	-0.378581	-0.097140
C	-1.091579	1.031859	0.027047
C	-0.680784	2.168843	0.237303
C	-0.283128	3.536333	0.515945
C	0.493270	-1.426976	-0.692906
C	1.321031	-0.336106	-0.628150
C	2.717099	-0.346633	0.025292
C	0.794354	0.890452	-1.126968
Cl	-3.543701	-0.168280	-0.782179
Cl	-1.882229	-1.168003	1.642273
C	2.713297	0.571699	1.268663
C	3.762903	0.167434	-0.991372
C	3.126496	-1.762995	0.464036
H	-1.016108	-0.879088	-2.104025
H	-1.376756	-2.336305	-1.162594
H	0.607342	3.577780	1.147845
H	-0.095693	4.091066	-0.407251
H	-1.098258	4.038522	1.046363
H	0.837723	-2.368927	-0.282694
H	1.369937	1.801452	-1.018797
H	0.141368	0.889529	-1.988153
H	3.701723	0.566495	1.736594

H	2.480860	1.608667	1.013319
H	1.983408	0.231171	2.007327
H	4.758417	0.169499	-0.538619
H	3.793937	-0.472355	-1.877701
H	3.549229	1.188478	-1.319309
H	4.135949	-1.734197	0.881769
H	2.461256	-2.161179	1.234471
H	3.138013	-2.461168	-0.377708

Energy + ZPE = -1374.570099 au.

Free Energy = -1374.613933 au.

TSD-m

1 imaginary frequency : -168.6 cm⁻¹

Cl	-1.067117	-1.569516	1.660485
B	-1.187991	-0.818685	-0.087426
C	0.265229	-0.760962	-0.856226
C	1.201125	0.341829	-0.446385
C	2.616808	-0.007463	0.023220
C	0.758752	1.622079	-0.519281
C	-0.563590	1.950810	-1.029833
C	-1.758124	0.631738	0.087359
C	-2.012549	1.829460	0.255451
C	-2.598885	3.082196	0.731224
Cl	-2.404621	-1.871262	-1.117377
C	3.424997	1.232358	0.447592
C	2.564117	-0.982314	1.222475
C	3.359060	-0.689143	-1.154805
H	0.015484	-0.633277	-1.916780
H	0.725480	-1.745020	-0.763938
H	1.357595	2.448367	-0.161441
H	-0.782336	3.012876	-1.107492
H	-0.909565	1.432166	-1.917362
H	-3.054363	3.639536	-0.090463
H	-3.371509	2.851899	1.467227
H	-1.840146	3.709630	1.204806
H	4.425913	0.922645	0.758877
H	3.540553	1.945305	-0.372950
H	2.961577	1.749354	1.292255
H	3.583408	-1.239863	1.524337
H	2.059921	-0.526803	2.078013
H	2.042158	-1.909441	0.982101
H	4.374071	-0.953854	-0.845129
H	2.858911	-1.604077	-1.478483
H	3.430700	-0.016303	-2.014028

Energy + ZPE = -1374.572152 au.

Free Energy = 1374.615483 au.

3

C	-0.904294	0.326578	0.032483
C	-0.915408	1.659178	-0.208398
C	-2.120352	2.479280	-0.585298
B	-2.158261	-0.569572	0.016478
Cl	-3.699835	-0.165666	0.809877
Cl	-2.115702	-2.190280	-0.729583
H	-3.038824	1.907114	-0.679845
H	-2.282990	3.271330	0.154948
H	-1.933608	2.983029	-1.540000
C	0.354079	2.472930	-0.155110
C	1.628503	1.681827	-0.111358
C	1.681551	0.365140	0.098209
C	0.402360	-0.405044	0.349222
C	2.990762	-0.441197	0.105770
C	3.025648	-1.383756	-1.122740
C	4.232952	0.466218	0.042691
C	3.083767	-1.291926	1.394838
H	0.291283	3.140407	0.719940
H	0.374653	3.158192	-1.012825
H	2.534898	2.253738	-0.272652
H	0.375706	-0.711189	1.404542
H	0.423835	-1.345957	-0.206699
H	2.199489	-2.098618	-1.118788
H	3.956710	-1.958825	-1.127746
H	2.975230	-0.811215	-2.053104
H	5.136876	-0.148336	0.072993
H	4.269567	1.158115	0.888722
H	4.264163	1.051759	-0.879901
H	2.279286	-2.027931	1.460230
H	3.040284	-0.660032	2.287088
H	4.031473	-1.838000	1.413864

Energy + ZPE = -1374.650951 au.

Free Energy = -1374.696053 au.

4

C	1.086861	-0.106527	-0.157113
C	0.378621	1.016806	-0.437104
C	0.943718	2.396268	-0.650757
B	2.606500	-0.170914	0.050399
Cl	3.503751	-1.655907	-0.378290
Cl	3.607959	1.097604	0.797157
H	0.447496	2.862427	-1.508210
H	0.725877	3.030900	0.216393
H	2.015426	2.416075	-0.825008
C	-1.121620	0.980851	-0.633479
C	-1.835868	-0.234677	-0.084805
C	-1.125340	-1.340393	0.146740
C	0.356191	-1.447531	-0.074180
C	-3.346423	-0.115010	0.158587
C	-3.983544	-1.465932	0.530234
C	-3.608164	0.873680	1.321374

C	-4.044046	0.411136	-1.118274
H	-1.313047	1.071229	-1.713980
H	-1.537098	1.902168	-0.209843
H	-1.605539	-2.240027	0.514783
H	0.553056	-2.021807	-0.991646
H	0.788448	-2.058060	0.726053
H	-5.060017	-1.336497	0.672762
H	-3.574326	-1.867428	1.461131
H	-3.837081	-2.210466	-0.257100
H	-3.221229	1.873465	1.109940
H	-3.143402	0.518447	2.245246
H	-4.684007	0.969664	1.497103
H	-3.691609	1.406215	-1.400220
H	-5.123355	0.479166	-0.953456
H	-3.873485	-0.261791	-1.964012

Energy + ZPE = -1374.652288 au.
Free Energy = -1374.696881 au.

5

C	1.086861	-0.106527	-0.157113
C	0.378621	1.016806	-0.437104
C	0.943718	2.396268	-0.650757
B	2.606500	-0.170914	0.050399
Cl	3.503751	-1.655907	-0.378290
Cl	3.607959	1.097604	0.797157
H	0.447496	2.862427	-1.508210
H	0.725877	3.030900	0.216393
H	2.015426	2.416075	-0.825008
C	-1.121620	0.980851	-0.633479
C	-1.835868	-0.234677	-0.084805
C	-1.125340	-1.340393	0.146740
C	0.356191	-1.447531	-0.074180
C	-3.346423	-0.115010	0.158587
C	-3.983544	-1.465932	0.530234
C	-3.608164	0.873680	1.321374
C	-4.044046	0.411136	-1.118274
H	-1.313047	1.071229	-1.713980
H	-1.537098	1.902168	-0.209843
H	-1.605539	-2.240027	0.514783
H	0.553056	-2.021807	-0.991646
H	0.788448	-2.058060	0.726053
H	-5.060017	-1.336497	0.672762
H	-3.574326	-1.867428	1.461131
H	-3.837081	-2.210466	-0.257100
H	-3.221229	1.873465	1.109940
H	-3.143402	0.518447	2.245246
H	-4.684007	0.969664	1.497103
H	-3.691609	1.406215	-1.400220
H	-5.123355	0.479166	-0.953456
H	-3.873485	-0.261791	-1.964012

Energy + ZPE = -1374.652288 au.
Free Energy = -1374.696881 au.

6

C	-0.724258	-1.259080	-1.137003
C	0.653185	-1.221675	-0.524749
B	-1.933696	-0.998746	-0.180774
C	1.480976	-0.169979	-0.524838
Cl	-3.526054	-0.585540	-0.850266
Cl	-1.840964	-1.219240	1.572878
C	2.874407	-0.189454	0.120373
C	1.046277	1.141747	-1.193384
C	-0.044198	1.822942	-0.489556
C	-0.945298	2.373641	0.093908
C	-2.031004	3.041597	0.804930
H	-0.911552	-2.266328	-1.544487
H	-0.818192	-0.589102	-1.997115
H	0.960461	-2.137049	-0.033589
C	3.180842	-1.527469	0.816961
C	3.952540	0.037300	-0.968000
C	2.972643	0.935221	1.179445
H	0.733475	0.940928	-2.224952
H	1.892267	1.826600	-1.276327
H	-1.718329	4.024981	1.167132
H	-2.353509	2.454036	1.669276
H	-2.899214	3.184538	0.155572
H	2.237172	0.786465	1.974747
H	2.807528	1.926002	0.749594
H	3.968589	0.934952	1.632468
H	2.463755	-1.742588	1.613535
H	4.176151	-1.483914	1.267606
H	3.173371	-2.363530	0.112510
H	4.947935	0.037110	-0.513746
H	3.830284	0.992352	-1.484543
H	3.920926	-0.759221	-1.716736

Energy + ZPE = -1374.605972 au.
Free Energy = -1374.653890 au.

References

1. R. F. W. Bader, *Atoms in Molecules. A Quantum Theory*, Oxford Science Publications, Clarendon Press, London 1990.
2. C. F. Matta and R. J. Boyd, *The Quantum Theory of Atoms in Molecules: from solid state to DNA and drug design*, Wiley-VCH, Weinheim, 2007.
3. C. S. López, O. N. Faza, F. P. Cossío, D. M. York and A. R. de Lera, *Chem. Eur. J.*, 2005, **11**, 1734-1738.
4. D. Cremer and E. Kraka, *Angew. Chem. Int. Ed. Eng.*, 1984, **23**, 627-628.
5. G. Merino, A. Vela and T. Heine, *Chem. Rev.*, 2005, **105**, 3812-3841.
6. P. L. A. Popelier, *Coor. Chem. Rev.*, 2000, **197**, 169-189.
7. R. F. W. Bader, T. T. Nguyen-Dang and Y. Tal, *Rep. Prog. Phys.*, 1981, **44**, 893-948.
8. M. M. Vallejos, N. M. Peruchena and S. C. Pellegrinet, *Org. Biomol. Chem.*, 2013, **11**, 7953-7965.